Fraser River Action Plan

CANADA'S GREEN PLAN
LE PLAN VERT DU CANADA

Canada

Plume Delineation of a Pulp and Paper Mill Outfall Using Airborne Multispectral Imagery and Rhodamine Dye

DOE FRAP 1994-23

Environment Canada Environnement Canada

Plume Delineation of a Pulp and Paper Mill Outfall using Airborne Multispectral Imagery and Rhodamine Dye

Gary Borstad, Mark Zacharias and Randy Kerr

G. A. Borstad Associates Ltd.
Suite 114 - 9865 West Saanich Rd
Sidney B.C. , Canada V8L 3S1

for
Fraser Pollution Abatement Office
Environment Canada
Conservation and Protection
Environmental Protection
224 West Esplanade
North Vancouver B.C. V7H 3H7

October 1994

Disclaimer

This publication contains the results of a project conducted under contract. The ideas and opinions expressed herein do not necessarily state or reflect those of Environment Canada.

ABSTRACT

Remotely sensed data from the Borstad Associates Ltd. Compact Airborne Spectrographic Imager (CASI) were acquired April 61993 over the Scott Paper Pulp and Paper Mill on the Fraser River, near Vancouver, British Columbia coinciding with a conventional *in situ* dye dispersion study conducted independently by Seaconsult Marine Research Ltd. of Vancouver (Seaconsult 1994). During airborne data acquisition rhodamine WT tracer dye was pumped into the pulp mill effluent discharge at a continuous rate for 29 hours. An *in situ* towed fluorometer measured dye concentrations throughout the injection period, while simultaneously collecting salinity, temperature and density measurements at various depths.

Although the aerial data acquisition took place under very poor west-coast winter imaging conditions, results indicate that the CASI imagery can be used to map dispersal of near surface mill effluent with a spatial resolution of 1 m and at concentrations down to the 0.2% dilution level. A lower limit of detection would almost certainly be achievable under more favorable weather conditions. The 0.2°/0 concentration is a higher limit of detection than *in situ* fluorometer measurements made at the same time, but the synoptic and complete surface picture of effluent dispersion provided by the imaging may offset this disadvantage. This technology has been demonstrated to be feasible, and has the potential to map and monitor the dispersal of dyed effluent discharged from pulp and paper mills as well as other industrial pulp and paper mills in Canada and abroad.

TABLEOFCONTENTS

LIST OF FIGURES

LIST OF TABLES

LIST OF PLATES

1.0 Introduction

Remotely sensed data have been successfully used in supplementing *in situ* dye studies for the purposes of mapping and modeling municipal and industrial effluent discharges into water bodies. (Danaher *et al.* 1992, Zalloum *et al.* 1993). Although the detection of fluorescent tracer dyes in the water column is limited to the near surface layers, remote sensing techniques can be used to examine a large area in two dimensions, in contrast to conventional point or transect sampling. Remotely sensed data can also provide a synoptic picture of the movement, dispersion and deposition of the effluent both over space and time, which may not be immediately evident using other methods. Although larger oufalls can be detected and monitored from space, the study of most industrial and municipal outfalls will require more frequent, detailed imagery, and are better examined using airborne methods such as aerial photography, video and multispectral imaging.

One promising technique for effluent detection and mapping is the use of airborne digital multispectral imagery, which has the spectral sensitivity required to map dye concentrations well beyond the threshold of aerial photographs and conventional video systems (Borstad & Hill 1989). Certain imagers also have the ability to examine very small spectral ranges, which is beneficial for the detection of fluorescent dyes (Danaher *et al.* 1992, Zalloum *et al.* 1993).

This study uses airborne digital data collected from the Compact Airborne Spectrographic Imager (CASI) to map a dyed effluent plume from the Scott Paper Pulp and Paper Mill on the Fraser River, near Vancouver, B.C. The over flights of the outfall coincided with an in *situ* dye dispersion study conducted independently by Seaconsult Marine Research Ltd. of Vancouver (Seaconsult 1994). Results from the *in situ* study were used to calibrate the airborne imagery for the purposes of synoptically mapping dye concentrations throughout a five hour period. The airborne derived dye concentrations were then used to monitor the movement and dispersion of the plume throughout the study period.

Results indicate that airborne measurements of the dye plume could map dye concentrations to 2 parts per billion (ppb) and therefore effluent concentrations to 0.2 %. Had the weather, and therefore illumination conditions been better, the effluent detection threshold could have been <0.1%.

2.0 Materials and Methods

2.1 Airborne instrumentation

The instrument used to acquire the airborne imagery was the Borstaad Associates Ltd. Compact Airborne Spectrographic Imager (CASI), an imaging spectrometer/mu ltispectral i mager sensitive in the 450 (blue) to 950 (near infrared) nanometre spectral regions (Borstad & Hill 1989). The instrument can collect imagery in up to 15 user defined spectral regions (bands), which can be programmed prior to the mission or at any time during the flight. The image swath of the instrument is 512 pixels, where the width of a pixel is dependent on flight height. In addition to the CASI, an onboard gyroscope and flux-gate compass provide pitch, roll and yaw information which is used in conjunction with GPS information to correct the imagery and project it into UTM coordinates (Zacharias et *a/.* 1994).

2.2 Dye Injection and Tidal Cycles

The *in situ* dye study was implemented by Seaconsult Marine Research Ltd. under separate contract (Seaconsult, 1994). Of particular interest was whether the effluent from a previous tidal cycle failed to disperse to safe levels and was transported back up the river during flood tide to add to the already high concentrations (also termed the double dosing effect). The study took place over one complete diurnal tidal cycle to gain an understanding of how the effluent disperses over time. Dye injection began at 1200 hrs PDT on April 6 1993 and tracking ended at 1600 hrs on April 7. The tidal states during imaging were derived from current projections done for the Lower Fraser River by Anne Woollard of the Institute of Ocean Sciences (10S), and areas follows: high water slack tide at 0800, low tide at 1515 and low slack tide at 1620 on April 6 (Figure 1).

A total of 90.4 L of Intracid Rhodamine WT liquid dye was pumped into the waste water stream of the Scott Paper Mill at a constant rate for 29 hours where the outflow discharge was approximately 180 Us. The dye concentrations were mapped *in situ* using Seaconsult's TRACER *Dragonfly* system, consisting of a Variosens fluorometer and SeaBird STD (salinity, temperature and depth). The system is mounted on an electro-mechanical towfish and is reported to be

vertically accurate to 5 cm and horizontally accurate to 5-10 metres using differential GPS (Seaconsult 1994). Transect spacing ranged from 15 to 50 metres, depending on the distance from the outfall and tidal state. The transects were not fixed prior to the study, rather the sampling boat assessed the state of the plume and adjusted the transects accordingly. Before the dye injection began, the fluorometer was used to determine the baseline, or background fluorescence, where the highest value recorded prior to dye injection was used as the baseline for the fluorometer calibration. As the Variosense fluorometer is accurate to 0.05 ug/L, the effluent plume could be mapped to 0.010/0 effluent concentration (Seaconsult, 1994).

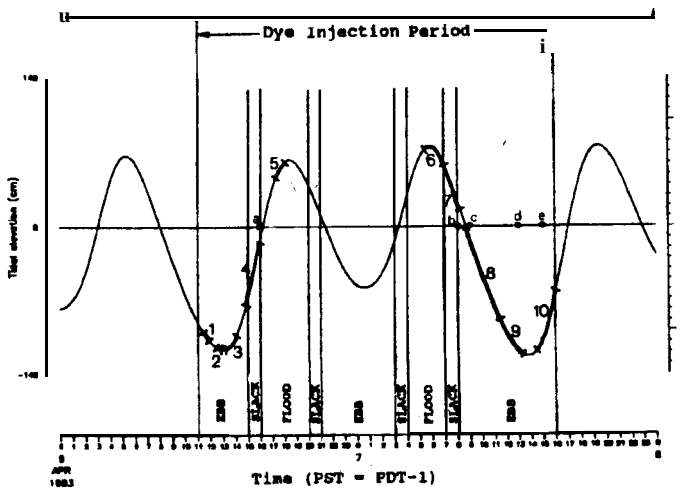

Figure 1. Tidal fluctuations and survey times for April 61993. Flights took place between 0900-1000, 1150-1231, 1424-1449 and 1558-1654 hrs PDT.

2.3. **Aerial Data Collection**

The mission was flown on April 61993 using a float equipped de Havilland Beaver chartered from Cooper Air Ltd. in Sidney, British Columbia. This aircraft was ideal for this study because of its size, slow speed, factory installed airphoto port and ability to operate in poor weather. Five flight lines were flown repeatedly throughout the day, covering the Scott Paper Mill and the surrounding regions as well as the South Arm of the Fraser River south west of Annacis Island (Plates 1- 2). As the date of the experiment was set several weeks prior

to the flight, the imaging was to proceed regardless of weather conditions. During the day of the flights, weather conditions were very poor - approximately 2 miles visibility in rain with moderate air turbulence and low cloud ceilings. Data were acquired at 300 m (1000) and 450 m (1500') altitude using a four channel and a twelve channel bandset (Table 1). The twelve channel bandset provided good spectral definition, but the longer instrument integration times required for 12 bands under such low illumination resulted in relatively poor ground resolution (approximately 4 m along track). This was noted by the operator during the flight and another configuration using much wider spectral bands was implemented. This 4 channel bandset provided the required sensitivity to acquire good signal at much shorter integration times and much better spatial resolution (approximately 1.5 m).

Although the mission was staged from Patricia Bay on Vancouver Island, the ' aircraft landed at the float-plane dock on the North Arm of the Fraser River after each flight Three subsequent flights were made later in the day corresponding with times of the tide and current extremes that would influence the oufalls and dye plume. The first flight occurred between 0900 and 1010 hours PDT to determine the background spectral qualities of the river. Data acquisition on the second flight began at 1150 and ended at 1231 hours and the third flight ran from 1424 to 1449 hours. The 'last flight started recording at'1 558 and ended at 1700 hours due to low solar angles and poor weather (Table 2).

Table 1. The twelve channel and four channel bandsets. Wavelengths are in nanometres (rim).

Band Number	Start	End	Width
Band 1	428.7	**456.7**	**28.0**
Band 2	476.0	**491.9**	**15.9**
Band 3	509.5	**527.2**	17.7
Band 4	541.4	**557.4**	**16.0**
Band 5	594.8	**602.0**	7.2
Band 6	632.4	**641.4**	9.0
Band 7	659.4	668.4	9.0
Band 8	672.0	684.6	12.6
Band 9	688.2	697.2	9.0
Band 10	700.8	711.7	10.9
Band 11	744.3	751.5	7.2
Band 12	839.0	855.4	16.4

Band	Start	End	Width
Band 1	**430.9**	**498.8**	**67.9**
Band 2	**509.3**	**590.4**	81.1
Band 3	**604.5**	**689.8**	**85.3**
Band 4	**709.4**	**759.4**	50.0

Table 2. April 6 dye study flights with dye arid tidal states.

	0800	**High Slack Water**
Flight 1	**0900-1010**	**Prior to dye** injection
	1200	Dye injection starts
Flight 2	1150-1231	Start of dye injection
Flight 3	1424-1449	Ebbing tide
	1515	Low tide
Flight 4	1558-1700	Slack tide
	1620	Low Slack water

2.4 Aerial Data Processing

Before the imagery can be analyzed, the data undergoes radiometric calibration and geometric correction. During radiometric calibration raw digital counts are converted to radiance units of uW/cm2/sr/nm using instrument responsivity calibration functions. Geometric correction uses roll, pitch and yaw information provided by a separate onboard gyroscope and a flux-gate compass which record aircraft attitude during data acquisition. Because the imagery for this study was acquired under low cloud in strong, gusty winds, there was a good deal of aircraft motion. Our correction procedures in early 1994 did not fully remove these effects and the geometry of the imagery presented here is slightly different in each image. Each pass occurred at a slightly different altitude and thus the image widths are different.

During this mission, autonomous GPS (Global Positioning System) information collected on the plane was used to project the imagery into a real world coordinate system. However, because of intentional scrambling of the GPS signal by the American military, the use of autonomous GPS (so called because only one GPS receiver is used) limits the positional accuracy of the geocorrected image to +/- 50 metres. This could theoretically have been reduced to +/- 10 metres if differential information was recorded.

Once the image data are calibrated and mapped, they can be directly compared with the *in situ* fluorometry data. For this study, paper hardcopy maps of the boat track were provided by Seaconsult. Since the boat traveled relatively slowly, it could not build a map of the dye plume synoptically, and fluorometer data from periods of up to two hours were plotted together to map the dye.

Several different maps for each time period were available, each showing that part of the boat track above a specified effluent concentration. These were matched with the image data to provide an empirical *in situ* calibration.

3.0 **Results**

3.1. Spectral signature of the Rhodamine dye

Rhodamine WT absorbs light in the vicinity of 550 nm and fluoresces at 600 nm. Figure 2 illustrates an upwelling spectrum of the dye and the surrounding river derived from a 12 band image acquired at 16:45. Excellent spectral definition of the plume is obtained using the bands at 600 and 550 nm.

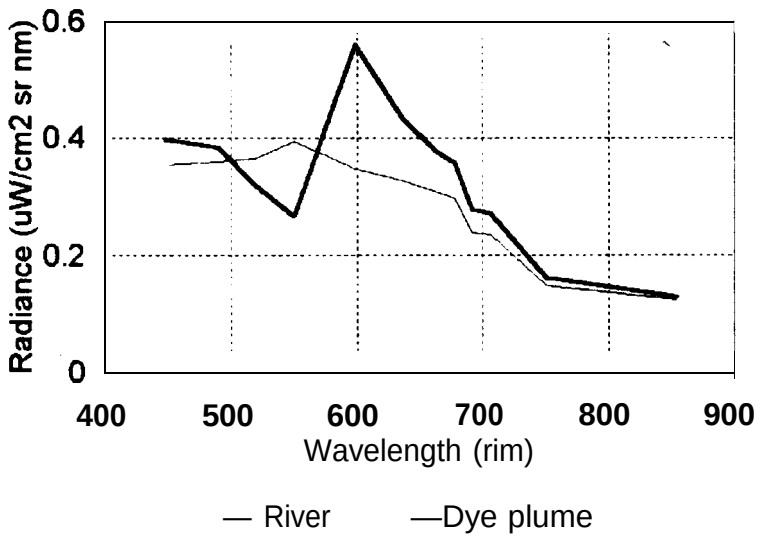

Figure 2. The spectrum of upwelling radiance from the dye plume and surrounding river water acquired with the 12 band set, showing the absorption by Rhodamine in the 550 nm band and fluorescence in the 600 nm band.

As outlined earlier, examination of the real-time display during flight showed that the 12 band configuration was giving very low signal levels, and when these were increased to give adequate signals, the spatial resolution was severely degraded. Not having the software ability in the aircraft to analyze the signals from the 12 band set and design an optimum 4 band set, the flight crew therefore chose to supplement the 12 band coverage with a generalized four ‘ band configuration normally used for other studies. While this band configuration was not optimal for the Rhodamine signature, it was more than

adequate to separate the dye from the surrounding river water. Figure 3 illustrates the spectrum of the dye and river water acquired using the 4 band set at 16:10.

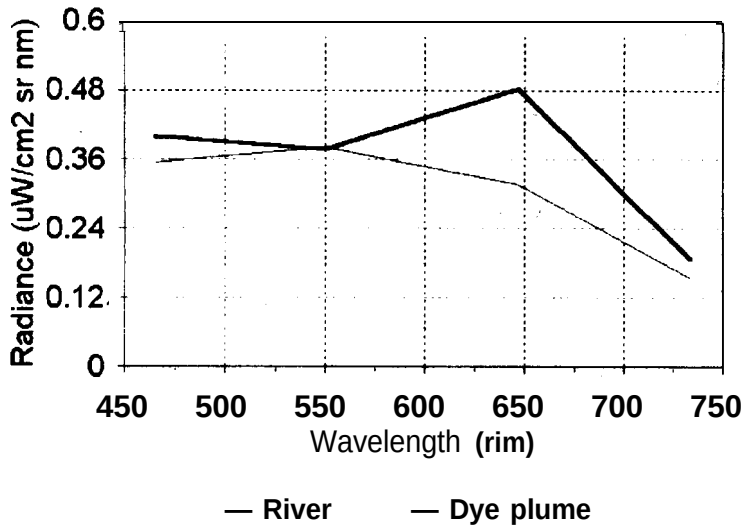

Figure 3. The spectrum of upwelling radiance from the dye plume and surrounding river water acquired with the 4 band set, showing the absorption by Rhodamine in the 550 nm band and fluorescence in the 650 nm band.

3.2. **Temporal changes in illumination and of spectral signatures**

Of the 57 image files acquired over various locations throughout the day, six images over the Scott paper outfall, spanning the period from just before dye injection at 12:00 hours to the last flight at 16:39 hours, were selected for this study (Plate 3). All images were collected with the four channel bandset with the exception of image 2 (at 12:22), as there were no four channel passes over the study area during the last half of flight 3, when the dye began to appear (the dye first appears in the imagery at 12:22). All six images have been calibrated in absolute radiance (uW cm2 sr nm) for analysis, therefore the changes in brightness between images is a result of changing illumination conditions throughout the day (Plate 3). The images acquired later in the day are darker due to lower solar angles and increasing cloud, with image 4 the darkest as the pass coincided with dense cumulus cloud shadows on the ground. As image 2 was acquired with the 12 channel bandset using narrower bandwidths, the lower signal levels result in a slightly darker image.

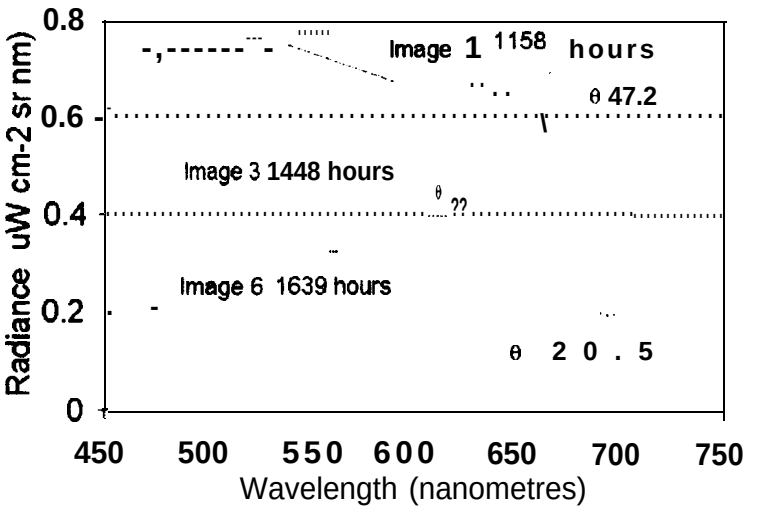

Figure 4. A radiance plot of river water (without dye) for Images 1, 3 and 6. Image 1 was acquired near solar noon and as a result is the brightest image. As solar elevation (θ) decreased and cloud cover increased, image brightness decreased.

Since our airborne method involves measuring the dye concentration by reflected and absorbed natural light, changes in illumination during the experiment can be expected to affect the measurement. Figure 4 and Plate 3 show that the illumination decreased throughout the imaging period, and Figure 5 illustrates that it also changed in spectral character. A comparison of the spectra of the river water from flight 4 with that from flight 1‘ in Figure 5 shows both the change in absolute amount of irradiance as well as the spectral character. As seen earlier, the upwelling radiance in image 1 was slightly more than twice that in image 6. There was also relatively more infrared signal at the time of the first flight than on the last flight of the day, but the other bands varied together showing that there was no change in colour of the river in the three shorter bands. These spectral differences are consistent with a small change in turbidity of the river during the study period.

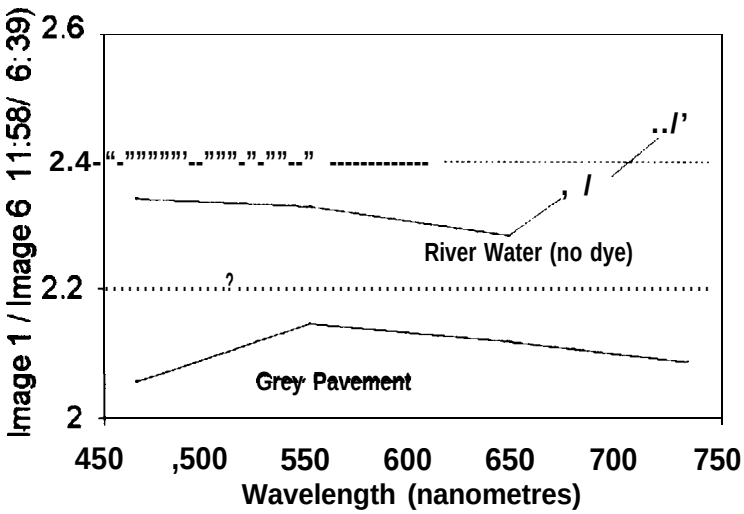

Figure 5. The ratio of upwelling radiance in Image 1 to that in Image 6 for areas of river water and gray pavement. The figure shows that the pavement at 1158 hrs was approximately 2.1 times brighter than 1639 hrs, whereas the river is abnormally bright, most likely due to changes in turbidity between the two times.

If there was an' increase in turbidity, it should also have caused an increase in brightness of the river. As another check on differences in both absolute illumination and its spectral character, we extracted the upwelling radiance spectrum from what should be a more constant target -9 paved road intersection near the study site. Figure 5 shows that the brightness of the paved area did not change as much as the river. Both the river and pavement show relatively small changes in bands 3 and 2. By normalizing the river spectra to the invariant pavement, we can create 'pseudo-reflectance' spectra which should have the changes in illumination removed (Figure 6) allowing us to compare dye concentrations between images taken at different times of the day. The fact that the river water has a higher reflectance in all bands in Image 1, and images 3 and 6 are nearly identical reinforces the suggestion that the river turbidity was greater at that time.

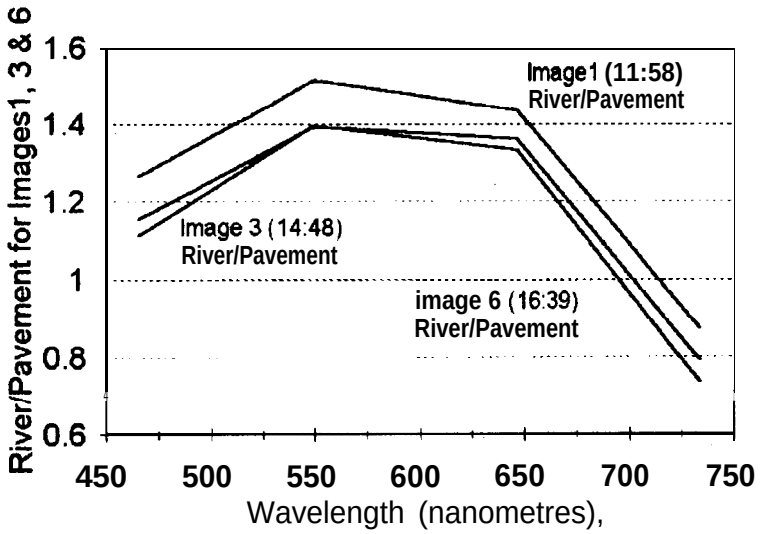

Figure 6. Three 'pseudo reflectance' spectra created by normalizing the spectra from a homogeneous area of river in each image by the signal from a nearby pavement area in the same image. The fact that the 'pseudo-reflectance' from the river was greater in Image 1 than in the later images suggests a greater turbidity at 11:58 than later in the day.

3.3. **Normalizing illumination differences using ratios**

As the illumination differences between scenes will have to be normalized before any calibration of the imagery can occur, simple red/green ratios were used, which normalized between scene illumination differences. The ratio for the four band imagery is

$$R_{3/2} = \lambda_{605 - 690nm} / \lambda_{509 - 590nm}$$

and the 12 band ratio is

$$R_{5/4} = \lambda_{595 - 602nm} / \lambda_{541 - 557nm}$$

where the resulting ratio image for each bandset (4 and 12 channel) will be different and have to be calibrated separately. Although there are other methods of normalizing the different images using more complex ratios and separating background signals from river and dye signals using cross correlation techniques (see Zalloum *et al.* 1993), simple ratios have proved effective for scene

normalization and dye calibration (Danaher *eta/.* 1992). The red / green ratios had the additional benefit of highlighting the red/green differences between the dye plume and surrounding water due to the fluorescence/absorption characteristics of these spectral regions.

3.4. **Calibration of airborne imagery in effluent concentration units**

in situ data for the calibration was taken not from the overall dye contour maps for specific periods throughout the day (Plates 4- 8), but the individual boat track plots with the dye concentration thresholds. The boat fluorometer maps were plotted on a transparency using the detection thresholds to draw contours on the mylar. This technique worked well for the files acquired during the last flight (tape 4), but there was only a single boat track to calibrate File 12 (12 band) therefore the calibration may not be as accurate as the others (Plate **4).** The other problem with the boat track data is that it often runs over land, which would indicate that the *in situ* maps may not be that accurate.

The Seaconsult flurometer data are measured in parts per billion (ppb) which is then converted to effluent concentration using the rate of effluent discharge, rate of dye input and background fluorescence of the river water. Dye concentrations are now given as the percentage of effluent in the river. Numerical values (averages and standard deviations) were extracted from 10 m by 10 m areas in the imagery coinciding with locations for which dye concentrations were available in the boat tracks. There is good agreement between the *in situ* dye data, and the red/green ratios from the airborne data. In Figure 7, the points represent pixel averages from the imagery corresponding to various effluent concentrations. A regression line (r^2=.94) has been calculated. The coloured boxes represent the colours assigned to the calibrated imagery (Plates **4- 8). The** width of the boxes represent the range of concentrations for that colour, while the vertical range shows the range of standard deviations . The dashed line is an extension of the regression line out of the range for which calibration data are available, to provide a prediction for high ratio values near the discharge point.

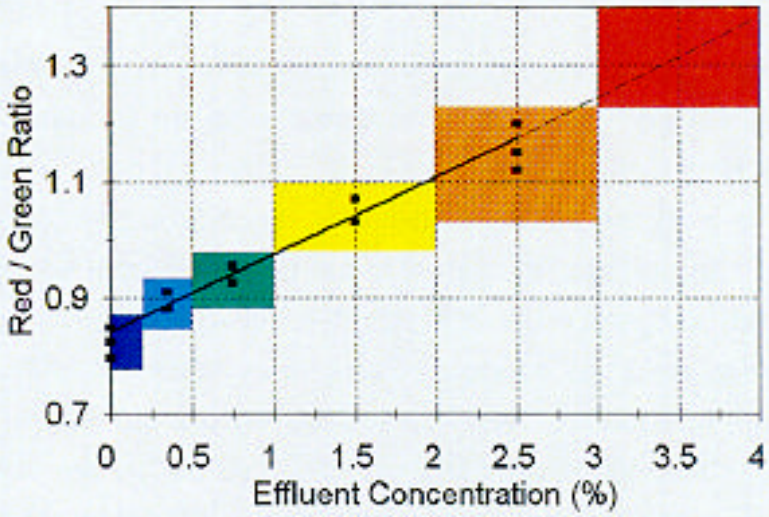

Figure 7. Effluent concentration verses the ratio (band 3/band 2) for images 3,4,5 and 6. r^2 = .94.

Image 2 which was acquired using the twelve channel bandset was calibrated separately. Figure 8 illustrates the calibration relationship for this image.

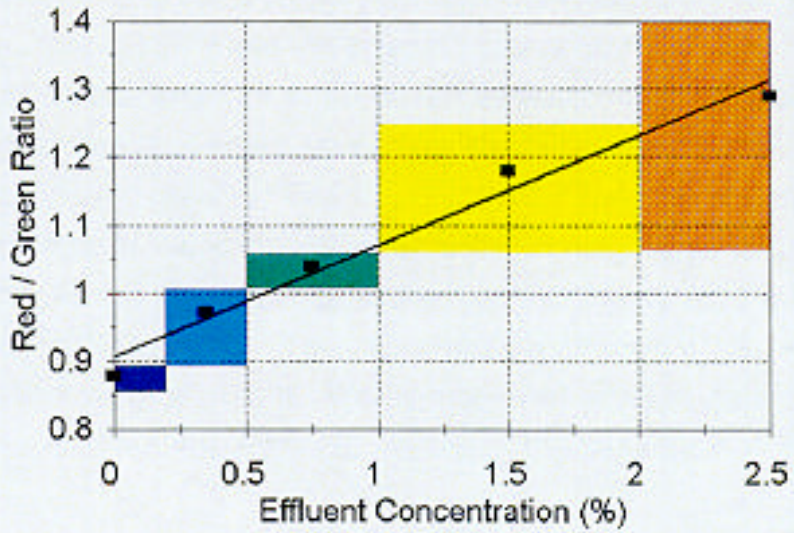

Figure 8. Effluent concentration versus the ratio (band5/band4) for 12:22 PDT (image 2). r^2 = .93.

4. Discussion

4.1. Calibration

While the plumes are well delineated in the imagery, the calibration in terms of effluent concentration is not as accurate as it could be. This is because the dye concentration data used for calibration is highly generalized over space and time. The slow-moving boat could not map the plume except over a relatively long time period, by moving in and out of the plume and up and down the river. Not having been collected solely for calibration of the imagery, the dye data were collected and collated in such as way as to produce complete stand-alone maps of the effluent. It was not always easy to delineate the edge of the plume in areas which were not visited by the boat. Changes in concentration during the two hour period for which the dye tracking data are collated are also not well represented.

Conversely, the airborne imagery for each pass over the study site was collected in less than a minute, and a complete two dimensional picture of the extent and variability of the plume in the imaged area is produced. Note however, that not all of the plume was imaged on each pass. This is because of the bad weather - the aircraft was flying very low and the imaged area is very narrow. It should also be pointed out that in such turbid river water, the aircraft is viewing a relatively thin surface layer, while the towed fluorometer resided between .5 and 1.5 metres depth. Vertical profiles carried out by Seaconsult showed little stratification in the river, but some small differences between 1 m depth and the surface layer could be expected (Seaconsult 1994). The limit of detection for the *in situ* measurements is lower by almost an order of magnitude than for the imagery, and the diluted effluent is detected much further down the river with the flourometer than in the imagery. This is probably a function of the very low , illumination at the time of the flight. We expect lower limits of detection under better conditions, but can not expect to approach the sensitivity of *in situ* fluorometry.

4.2. The Temporal Sequence of imagery

4.2.1. Image 1 (11:58 PDT)

Image 1 was acquired just as the dye injection began, and no dye is yet visible, although effluent from some mills can be easily tracked without dye (Borstad 1993). However, while digital enhancements of this and other early images did not show a plume from Scott paper itself, an oily slick was visible emanating from combined sewer overflows just to the east of the Scott Paper outfall. The river in Image 1 is about 9.5% brighter than the other images when normalized with homogeneous pavement. Assuming the pseudo-reflectance normalized the illumination differences between images, this implies that the river was more turbid at noon than later in the day. Note that in this 4 band imagery, the 1.5 m resolution is sufficient to clearly show individual trees, pilings in the river and the details of features on land.

4.2.2. Image 2 (12:22 PDT)

Image 2 was acquired 20 minutes after the beginning of the pumping. Considerably less detail is visible in this twelve band imagery as pixels are mapped at 4 m resolution and individual trees, pilings and log booms in the river are not as clearly evident. Although it was acquired with the twelve channel bandset and the width and centre wavelengths are different, the image can be calibrated separately using the in *situ* flurometer data collected at that time (Plate 4). Both the imagery and fluorometer data (from depths of between 0.5 and 1.5 m) correlate well. The effluent is shown emanating from a small point source and spreading out downstream (to the south-west) in a narrow plume. The imagery accurately shows the turbulent nature of the billows along the edge of the plume.

4.2.3. Image 3 (14:48 PDT)

Image 3 was acquired at 14:48 hours - at low tide while the tide was still ebbing strongly, using the four channel bandset (Plate 5). *In situ* measurements were made between 13:55 and 15:11 much farther downstream of the mill than the previous sample period in order to track the transport of effluent to the limits of detection. Although there are no *in situ* measurements adjacent to the mill which

can be used for direct calibration of the imagery, we apply the calibration derived from images 4,5 and 6. The image data and towed fluorometry measurements are consistent with each other. The combination of river discharge and ebb tide was transporting the effluent rapidly downstream, with limited opportunity for the effluent to spread out on the surface. As a result, dye concentrations in the image are low near the mill, although the plume has extended to the north bank of the river.

4.2.4. Image 4 (16:10 PDT)

Image 4 was acquired at 16:10 hours, on a rising tide near the beginning of slack water (Plate 6). Coincident fluorometry data for this and the following two images were acquired from 15:49 to 17:06 hours. The shape of the plume in these three image differs rather markedly from the distribution shown by the in *situ* observations. This is almost certainly because of the very different time intervals over which the maps are made: the images are nearly synoptic, acquired over a minute or less, while the fluorometer map is a compilation of boat tracks over a 77 minute period. Considerable change in the plume dynamics would be expected over such a long time period, especially during slack water when the plume is being allowed to boil to the surface. The steep concentration gradient on the east side of the plume is similar for both the airborne and ship borne measurements as is the plume concentrations to the west.

At 16:10, the image data shows that concentrations near the discharge point have begun to increase. While the maximum effluent concentration was in the range 0.5-1 % at 14:48, by 16:10 there was a small area of more than 2% visible. A substantially larger area of 0.5- 1% was also visible. This increase in concentrations and the more sinuous nature of the plume are consistent with a slower downstream movement and less dilution at the later time.

4.2.5. Image 5 (16:19 PDT)

Image 5 was' acquired 9 minutes after image 4 (Plate 7). The plume at 16:19 was wider than earlier, with a smaller area of 0.5-1 -1% effluent and larger areas of higher concentrations. Concentrations near the discharge point had continued to increase, surpassing 3°/0. The more bunched nature of the plume is

expected during a slack tide, when the river and tide are not reinforcing each other.

4.2.6. Image 6 (16:39 PDT)

Image 6 was acquired at 16:39 hours, twenty minutes after image 5, but still during a rising tide and slack water (Plate 8). The downstream area of the plume is approximately the same size as in the earlier image, but the area of high concentration near the discharge point has continued to increase. The area of effluent concentration greater than 3% is greatest in image 6 (Table 3).

Table 3. Area in square meters of the effluent plume greater than a specified concentration

Time	Effluent Concentration in m^2.				
	0.2 - 0.5%	**0.5 - 1.0%**	**1.0 - 2.0%**	**2.0 - 3.0%**	**> 3.0%**
12:22	1645	1474	245	110	0
14:48	5087	225	0	0	0
16:10	6111	3843	457	198	0
16:19	11511	1305	644	414	81
16:39	5663	2464	509	794	162

5.0 Conclusions

This work has demonstrated that airborne multispectral imagery can be used to map effluent concentration from an industrial or other discharge via *in situ* calibration with Rhodamine dye. The imagery correlated well with *in situ* fluorometry and also provided detailed synoptic two dimensional information on the movements of effluent in the water column. This was accomplished in spite of very poor survey conditions (moderate air turbulence and low, variable light conditions). The airborne technique only produced data during daylight hours, and the lower limit of detection for the imagery was approximately 0.2% effluent for this data set (an order of magnitude higher than *in situ* measurements), but this might be expected to be lower with spectral bands which exactly matched the dye spectrum, better survey conditions and *in situ* measurements which were

more coincident with the airborne data. In fact, for experiments conducted in daytime and which relied on the imagery as the primary mapping tool, a much smaller and less expensive *in situ* sampling program would be required.

6.0. References

Borstad, G.A. and D. A. Hill, 1989. Using visible range imaging spectrometers to map ocean phenomena. *Proceedings from the Advanced Optics/ Instrumentation for Remote Sensing of the Earth's Surface from Space.* Vol. 1129.

Borstad, G. A. 1994. Aerial remote sensing of effluent plumes. Environmental Effects Monitoring, 20th Annual Aquatic Toxicity Workshop, Quebec, October 21, 1993.

Borstad, G. A., R. Kerr and L. Armstrong 1994. Combined sewer outflow mapping using an imaging spectrometer. A report to Environment Canada, Conservation and Protection 224 West Esplanade North Vancouver BC V7M 3H7.

Danaher, S. E O'Mognain and J. Walsh. 1992. A new cross-correlation algorithm and the detection of rhodamine-B dye in sea water. *International Journal of Remote Sensing,* 13(9):1743-1755.

Seaconsult Marine Research Ltd. 1994. Plume Delineation Study of the Scott Paper Outfall, Unpublished report to Environment Canada, Conservation and Protection 224 West Esplanade, North Vancouver BC V7M 3H7.

Zacharias, M. A., S.A. Akenhead, G.A. Borstad and R. Kerr, 1994. Three dimensional gee-referencing of airborne multispectral data for use in a GIS. *Symposium Proceedings GIS* 94, Vancouver, B.C.

Zalloum O. J. O'Mongain, J. Walsh, J. Danaher, S. Stapleton. 1993. Dye concentration estimation by remotely sensed spectral radiometry, *international Journal of Remote Sensing* **14(12) 2285-2300**

7.0 Acknowledgments

George Derksen of Environment Canada provided valuable assistance in arranging this project. Seaconsult Marine Research Ltd. kindly provided copies of their in situ flurometer data with which the aerial imagery could be calibrated.

Dr. Grant Bracher, Dave Hill, Scott Akenhead and Kyle Robinson assisted in various aspects of the study.

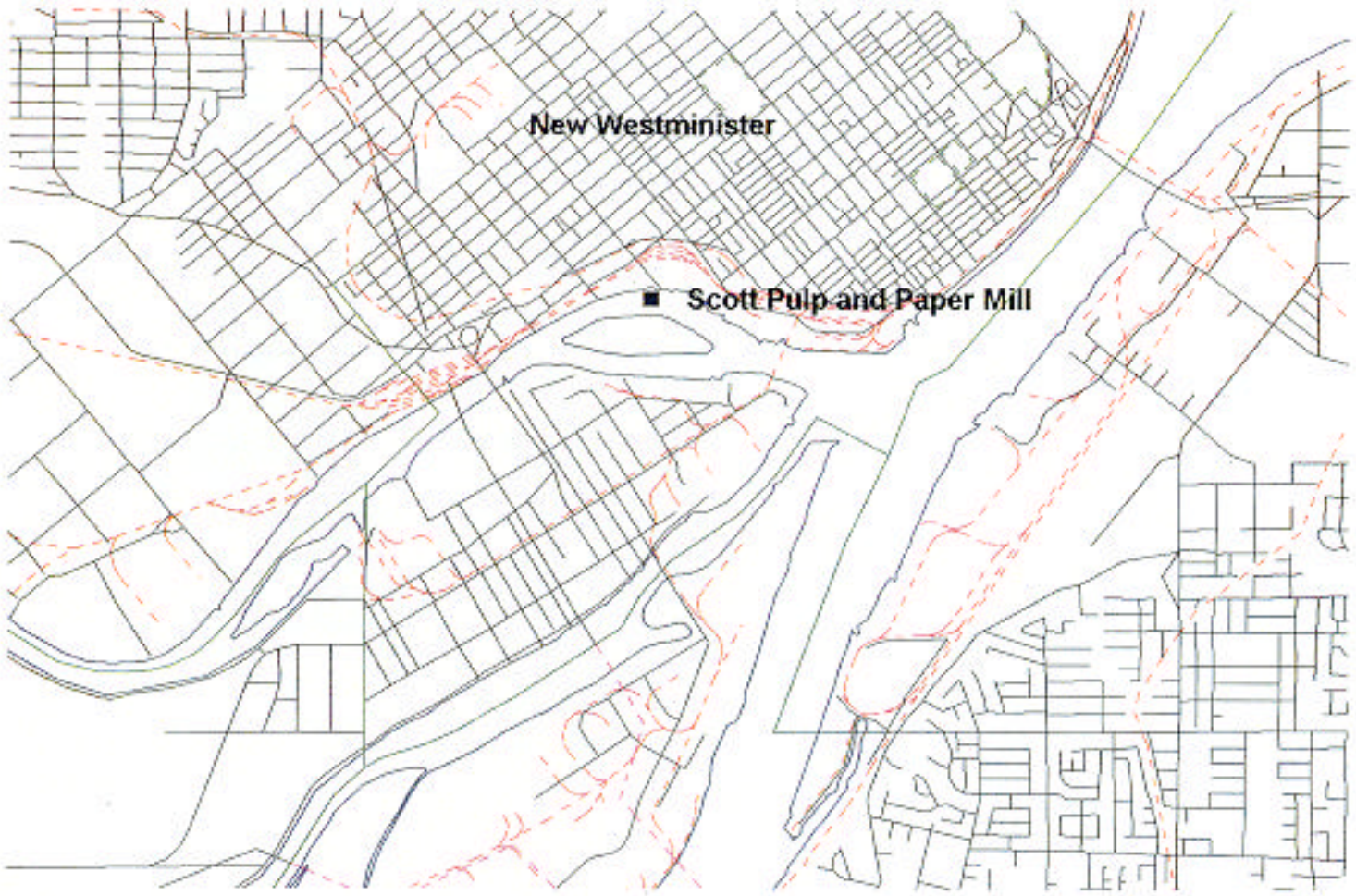

Plate 1. Location of the Scott Paper Mill on the North Arm of the Fraser River. The outfall location is denoted by the filled square.

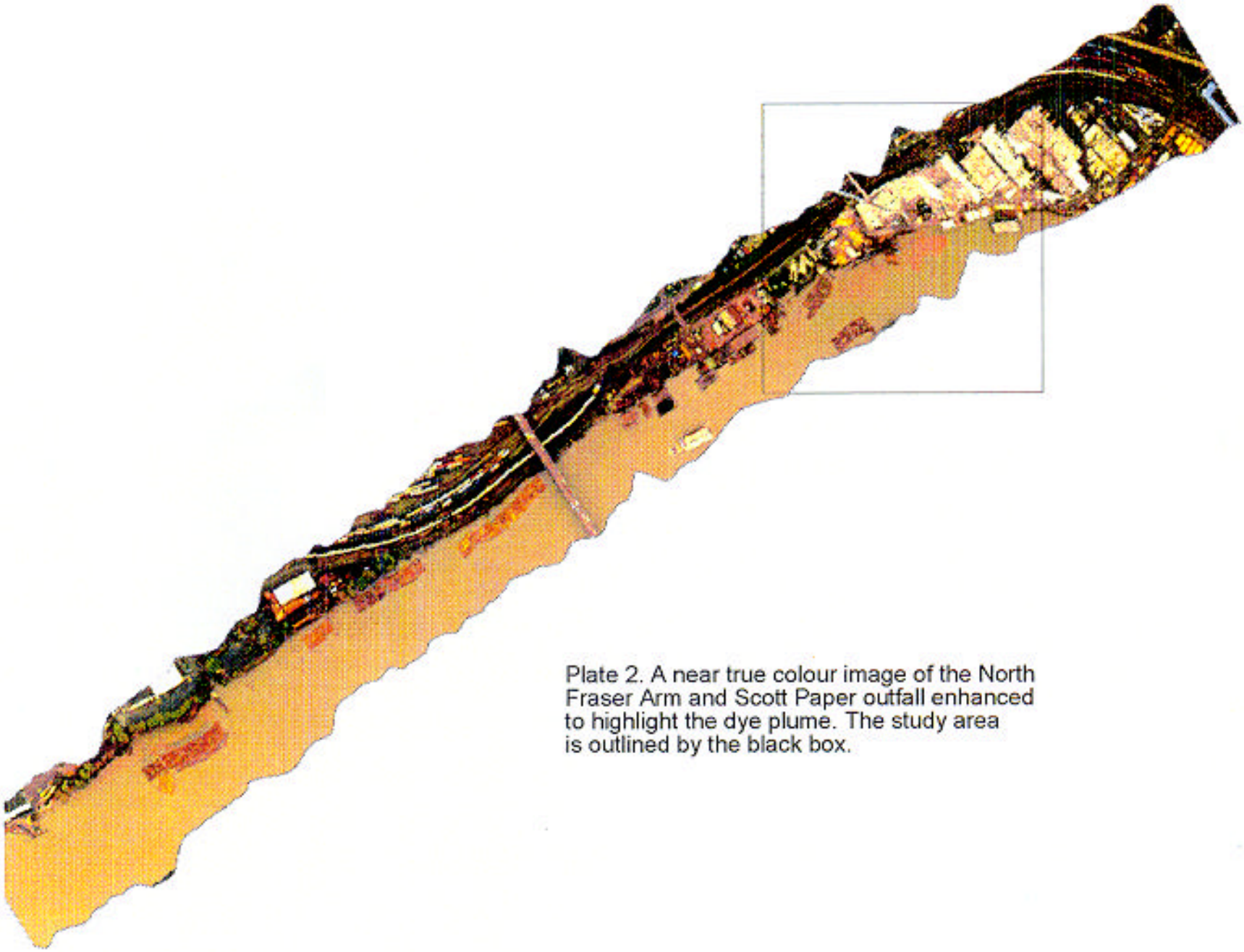

Plate 2. A near true colour image of the North Fraser Arm and Scott Paper outfall enhanced to highlight the dye plume. The study area is outlined by the black box.

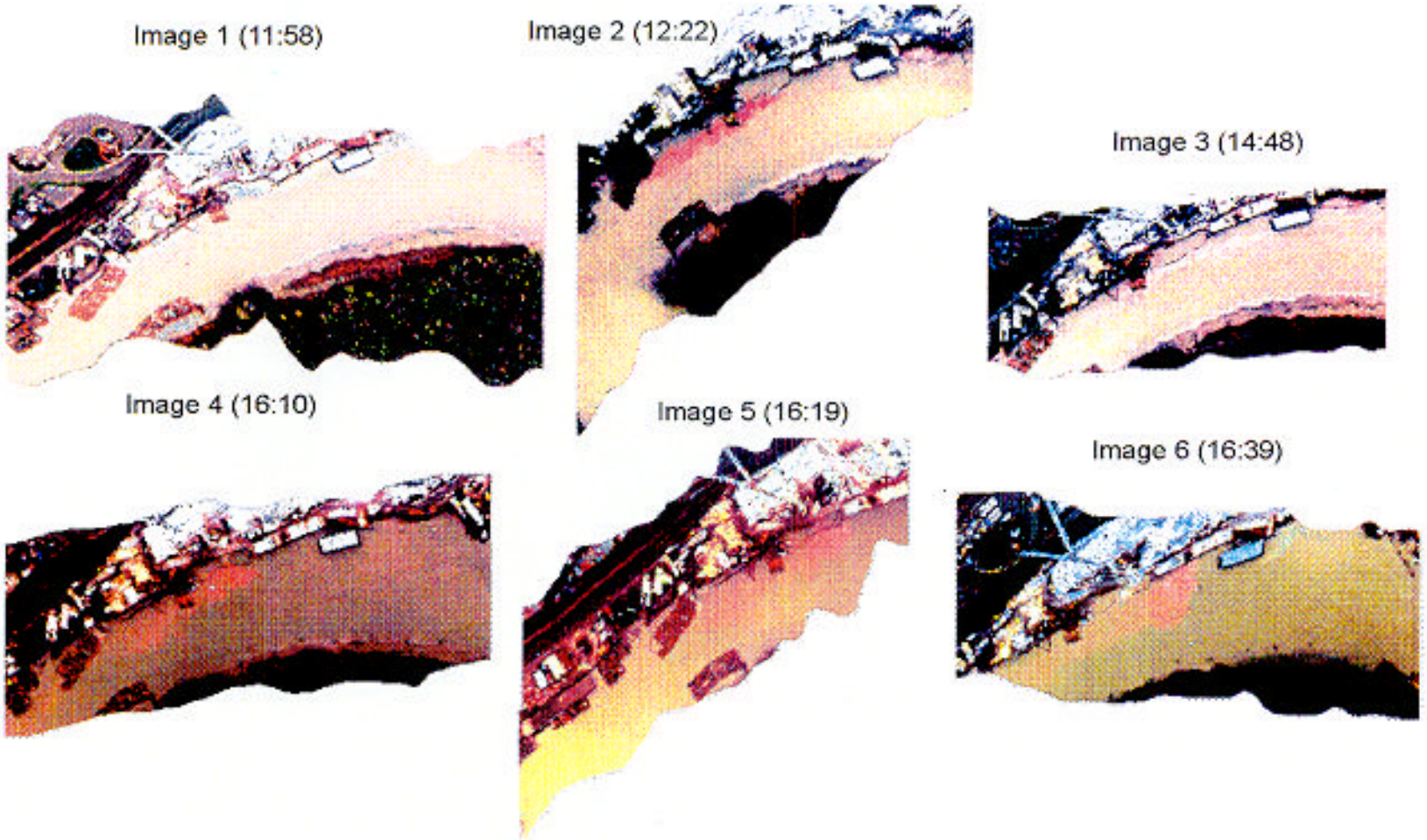

Plate 3. Near true colour images for the Scott Paper outfall. The images have been stretched to highlight dye concentrations in each image rather than maintain radiometric properties.

Plate 4. Calibrated CASI image of band 4 (red) / band 3 (green) using the 12 channel bandset and in situ fluorometer measurements. Imagery was acquired at 12:22 (PDT). Fluorometer measurements were acquired between 12:29 and 12:39.

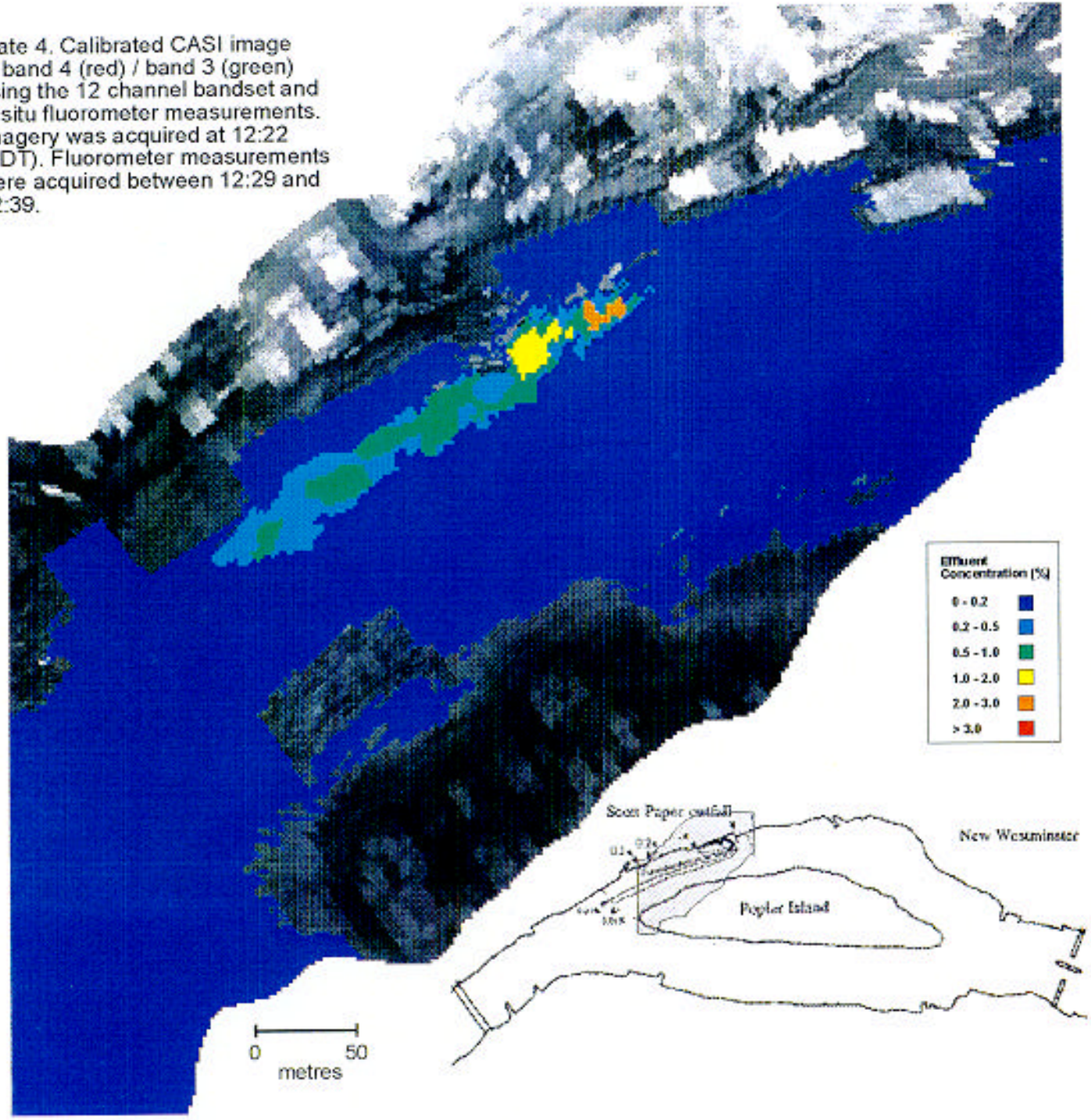

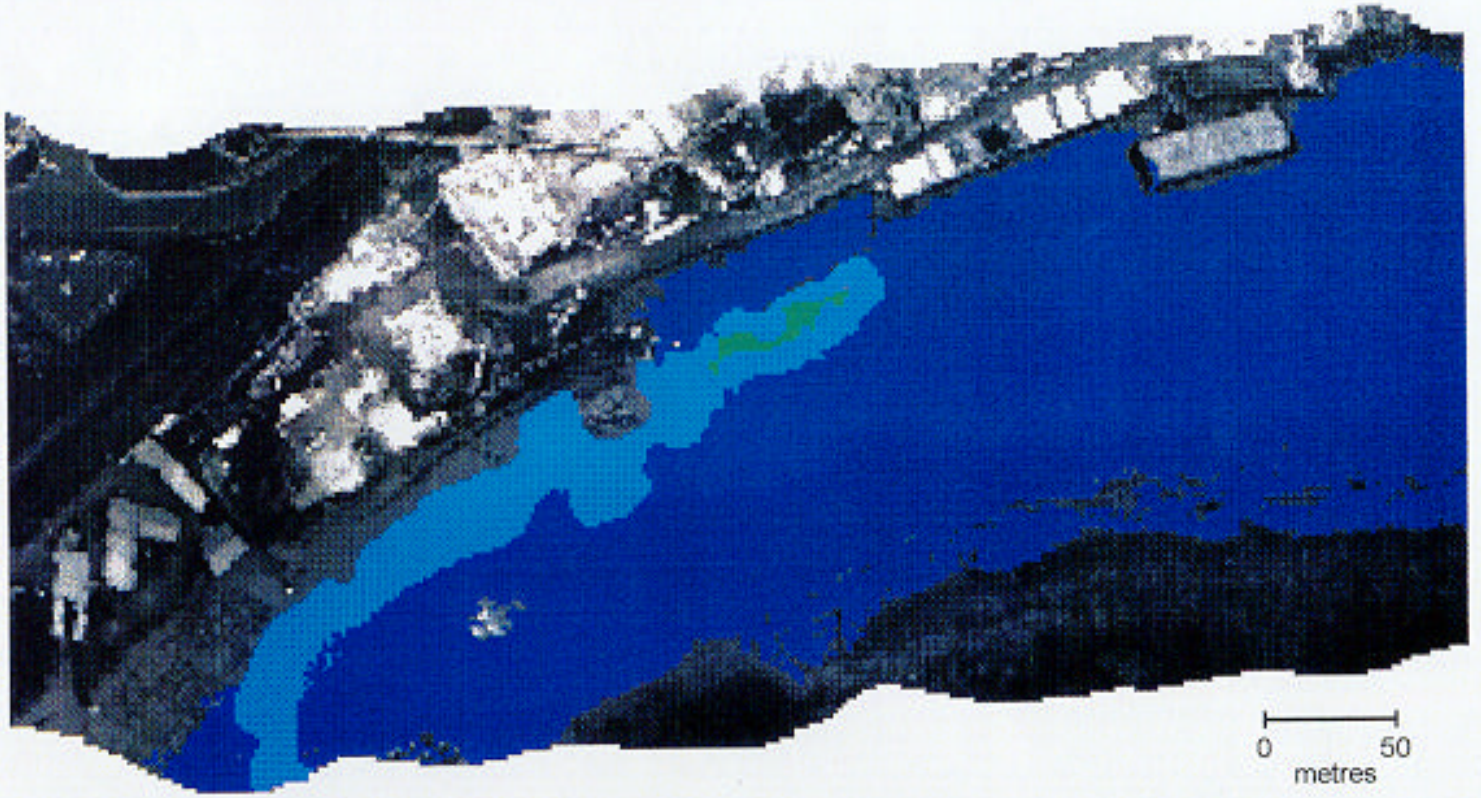

Plate 5. Calibrated CASI image of band 3 (red) / band 2 (green) and in situ fluorometer measurements.Imagery was acquired at 14:48 (PDT). Fluorometer measurements were acquired between 13:55 and 15:11.

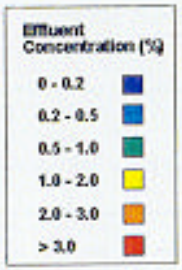

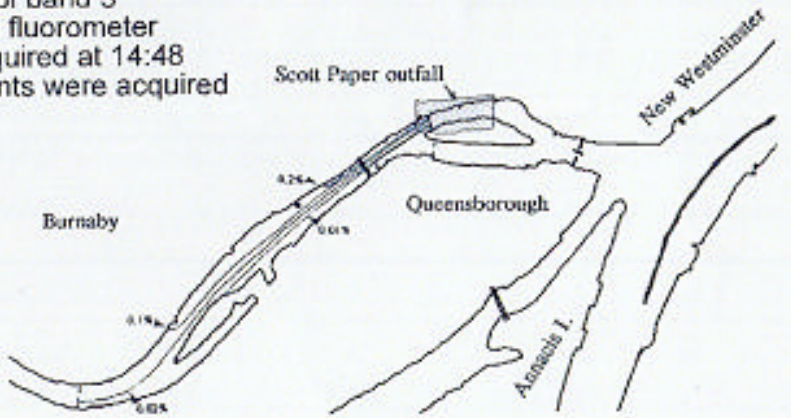

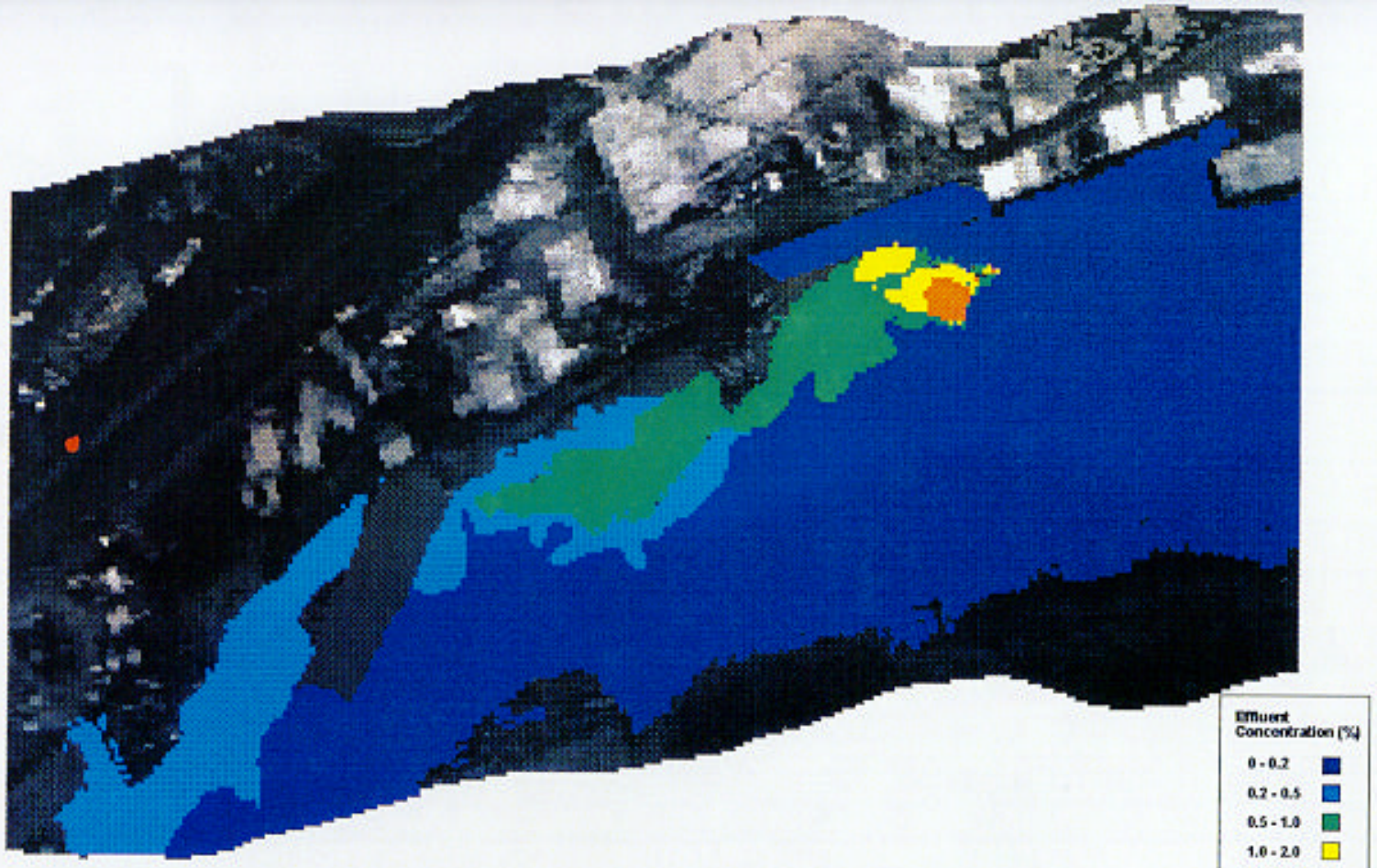

Plate 6. Calibrated CASI image of band 3 (red) / band 2 (green) and in situ fluorometer measurements. Imagery was acquired at 16:10 (PDT). Fluorometer measurements were acquired between 15:49 and 17:06.

0 50
metres

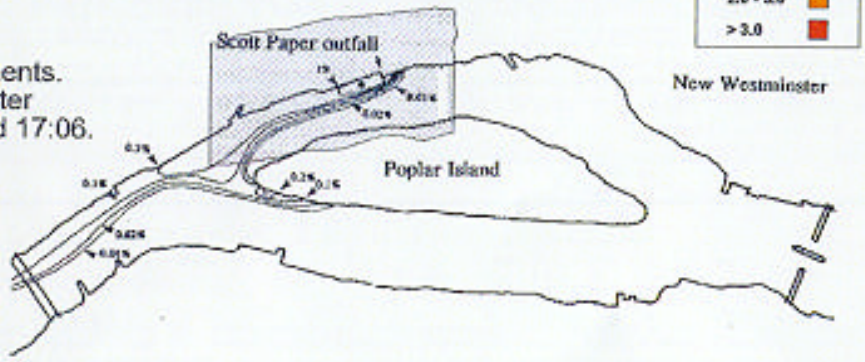

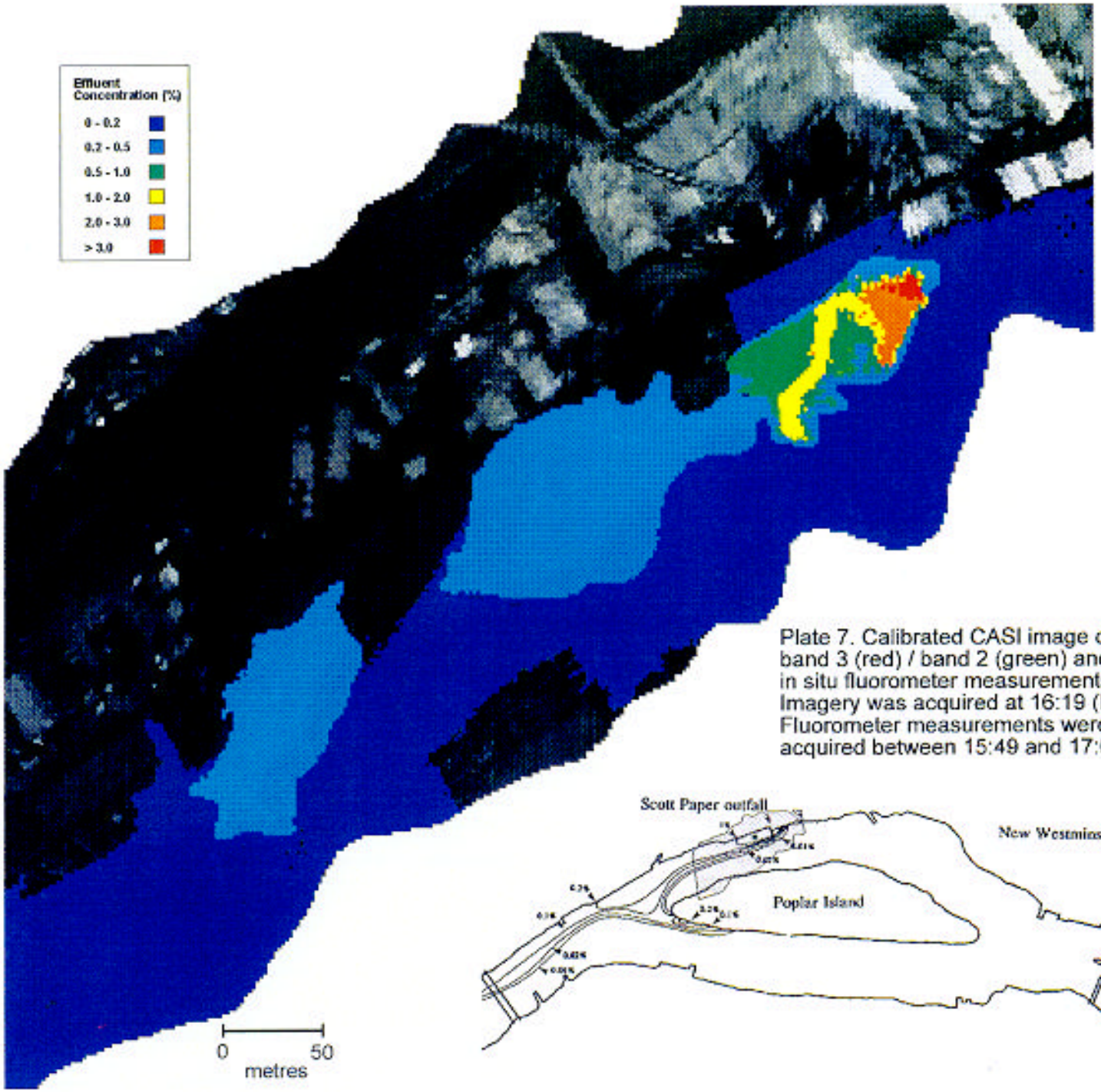

Plate 7. Calibrated CASI image of band 3 (red) / band 2 (green) and in situ fluorometer measurements. Imagery was acquired at 16:19 (PDT). Fluorometer measurements were acquired between 15:49 and 17:06.

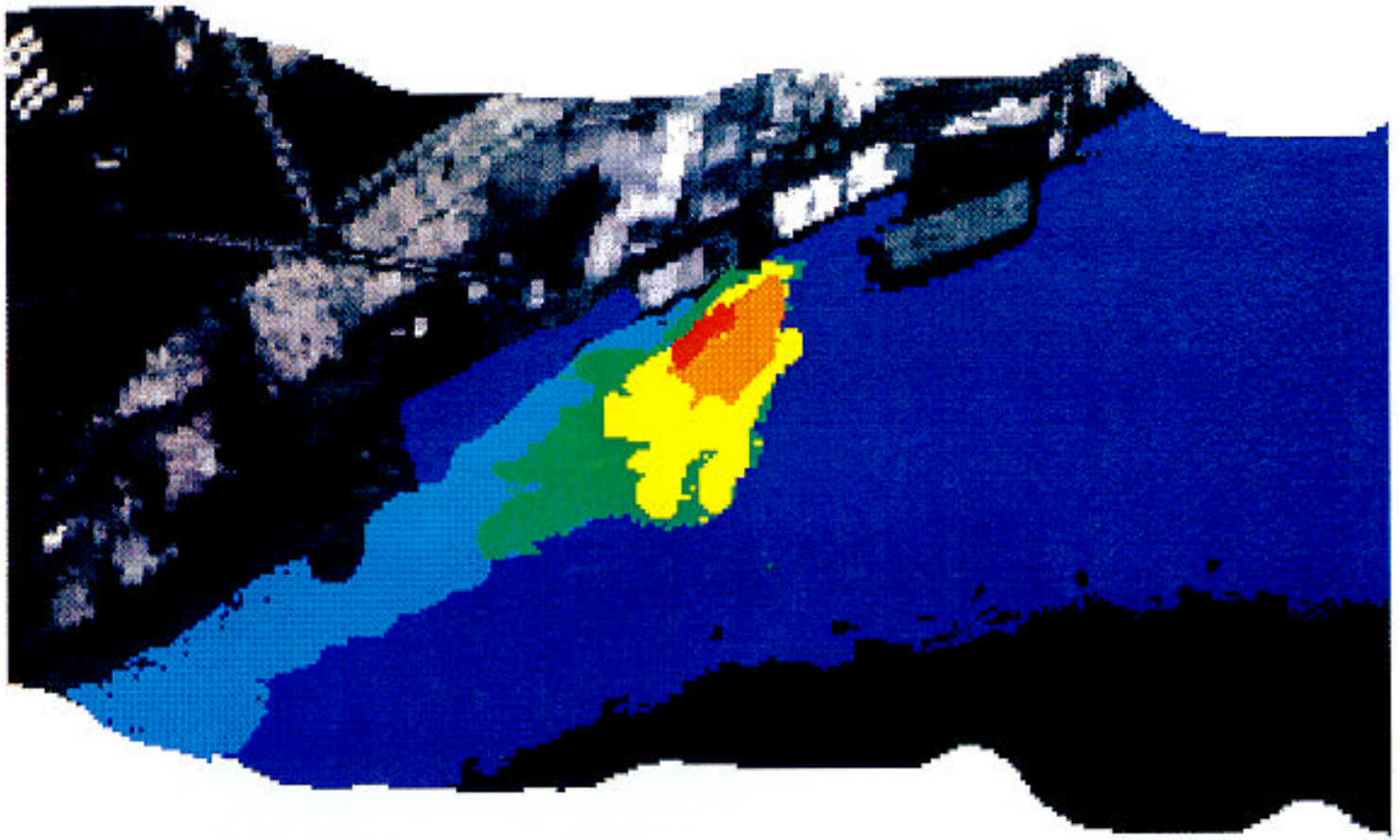

Plate 8. Calibrated CASI image of band 3 (red) / band 2 (green) and in situ fluorometer measurements.Imagery was acquired at 16:39 (PDT). Fluorometer measurements were acquired between 15:49 and 17:06..